ROBUST TRACKING CONTROL OF A SINGLE-LINK FLEXIBLE MANIPULATOR

M. L. Kerr[*], S. F. Asokanthan[*] and S. Jayasuriya[**]

[*] *Department of Mechanical Engineering, The University of Queensland, Brisbane, Queensland, 4072, Australia, E-mail: kerr@mech.uq.edu.au, sasokanthan@eng.uwo.ca*
[**] *Department of Mechanical Engineering, Texas A&M University, College Station, Texas, 77843, USA, E-mail: sjayasuriya@mengr.tamu.edu*

Abstract: Quantitative Feedback Theory (QFT) is employed to achieve time domain specifications on the tip position of a hybrid actuated single-link flexible manipulator. The manipulator payload conditions are varied to assess the robustness of the synthesised control system to parametric uncertainty. A combination of QFT multi input multi output (MIMO) design methods 1 (non-sequential) and 2 (sequential) is utilised in the control system synthesis to overcome difficulties in the construction of the performance bounds. Time domain simulations validate the design method and demonstrate the effectiveness of the control system that incorporates hybrid actuation. *Copyright © 2002 IFAC*

Keywords: Flexible Arms; Robust Control; Robotic Manipulators; MIMO; Multivariable Control; Feedback Control

1. INTRODUCTION

This paper presents a robust Quantitative Feedback Theory (QFT) control system for a single-link flexible manipulator. Flexible manipulators permit increased operational efficiencies through lower inertia and energy consumption. The primary challenge in their application is the coupled rigid-flexible dynamics and the resulting degradation of system stability and end-point tracking performance. A QFT based control system with hybrid actuation is proposed to address these challenges.

Numerous actuation techniques and control methodologies have been proposed for the control of flexible manipulator systems. Distributed actuators have been successfully employed for active vibration control of flexible beams (see, e.g. Yang and Liu, 1995). The inclusion of a discrete actuator gives rise to a multi input multi output (MIMO) system with coupled rigid-flexible dynamics. To overcome the adverse effects of the coupled rigid-flexible dynamics, a hybrid actuator control scheme (HACS) that employs a discrete actuator to primarily achieve the desired angular rotation and a distributed actuator

to suppress the undesirable link vibration is employed. HACS have been applied recently to both single and multi-link flexible manipulators resulting in reduced rest-to-rest slew times (see, e.g. Gu and Asokanthan, 1999). Non-robust controller synthesis techniques have been extensively applied to flexible manipulator systems (see, e.g. Book, 1990). Their performance is limited due to the inherent uncertainty in flexible manipulator systems.

The QFT synthesised control system is designed to achieve robust performance over a specified region of plant uncertainty that is characterised by the payload variation. The effectiveness of QFT for flexible manipulator control has been demonstrated previously by researchers Chang and Jayasuriya (1995) and Choi, *et al.* (1999). The present research utilises the MIMO QFT methodologies, with the control system synthesised to satisfy quantitative time domain specifications on the coupled MIMO system.

2. DYNAMIC MODELLING

The flexible manipulator and sensor-actuator pairs used in the present study are shown in Fig. 1. The

flexible manipulator model conforms to the UQ_ARM, an experimental test-bed at the University of Queensland (Gu and Asokanthan, 1999). In their study details of system parameter values and the development of the linearised model and matrix transfer function (MTF) are described. One exception to the model is that the two flexible modes considered in the present controller design have nonzero damping ratios, with a damping ratio of 0.005 for mode 1 and 0.001 for mode 2. The manipulator consists of a single flexible link with 2 inputs, the input voltage to the DC motor $V_a(t)$ and to the piezoelectric film $V_f(t)$, and 2 outputs, the hub angle $\theta(t)$ and the tip deflection $y_T(t)$, and is therefore a 2×2 MIMO system. The transverse elastic deformation is represented by $w(x,t)$.
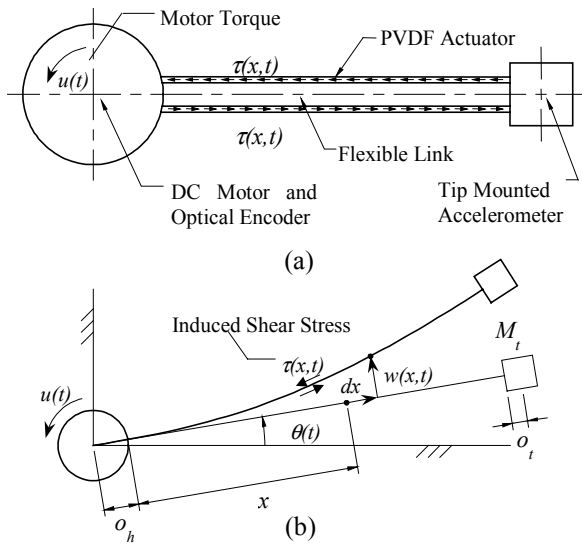
Fig. 1. Schematic of the Single-link Flexible Manipulator (Not to Scale)

The single-link flexible manipulator has parametric and non-parametric uncertainty that can be attributed to simplifications in the modelling of the system, unknown external disturbances and variations in the operating configuration. In this research only parametric uncertainty is considered. The uncertainty is introduced by varying the tip mass M_t of the manipulator and is characterised in the controller design by considering five values for M_t,

$$M_t \in [0, 0.018, 0.036, 0.054, 0.072]\,\text{kg} \quad (1)$$

This results in five plants that characterise the variation in dynamics of the manipulator, termed plant1 to plant5, plant5 having the largest tip mass.

3. QFT CONTROL OF THE MANIPULATOR

QFT is employed to synthesise a control system to satisfy quantitative time domain specifications imposed on the MIMO flexible manipulator system. The QFT synthesis procedure requires the translation of the time domain specifications into frequency domain specifications and the synthesis of the

controller and prefilter. Detailed explanations of the MISO and MIMO QFT synthesis procedures can be found in several references (see, e.g. Horowitz, 1991; Houpis and Rasmussen, 1999).

Throughout the present paper, the following concise transfer function notation is employed: the DC gain is represented by a constant in the numerator without parenthesis, poles and zeros at the origin are represented as (0), and simple nonzero poles and zeros and complex conjugate nonzero poles and zeros are represented as,

$$(\omega) \Rightarrow [(s/\omega)+1], \quad [\zeta : \omega] \Rightarrow [(s/\omega)^2 + (2\zeta s/\omega)+1]. \quad (2)$$

3.1 Time Domain Specifications

The performance requirement is a rest-to-rest slew to be completed within five seconds. The system is considered to have completed the slew when the hub angle error (θ_e) is less than 0.02 radians and the tip displacement $y_T(t)$ is less than $0.001\,\text{m}$. These requirements are related to the step response figures of merit on the outputs of the system, being the hub angle $\theta(t)$ and the tip displacement $y_T(t)$. The time domain specifications are:

S1: The hub angular response $\theta(t)$ should be stable, settle in five seconds and have an overshoot $\leq 2\%$. This is expressed as:

Overshoot: $\qquad Mp_1 \leq 2\%$
Settling Time: $\qquad T_{s1} \leq 5\,\text{s} \qquad (3)$

S2: The tip displacement $y_T(t)$ is required to be stable, reject the cross-coupling disturbance and settle in five seconds. This is expressed as:

Tip Displacement: $\qquad \max_{P\in\{P\}} y_T \Big|_{t\geq5\,\text{s}} \leq 0.001\,\text{m}$

Settling Time: $\qquad T_{s2} \leq 5\,\text{s} \qquad (4)$

3.2 MIMO QFT

The application of the QFT design methodology to a coupled 2×2 MIMO system requires the MIMO system to be converted into equivalent multi input single output (MISO) systems. The cross-coupling from the off-diagonal elements in the plant MTF become equivalent disturbance inputs to the MISO systems. The conversion is performed using the so called MIMO QFT design method 2 (Houpis and Rasmussen, 1999). The QFT MISO design methodology is then used to synthesise controllers and prefilters for the equivalent MISO systems that guarantee satisfaction of the quantitative time domain specifications on the original MIMO system.

The control structure is comprised of two feedback loops, loop1 from θ_r to θ and loop2 from y_r to y_T. The plant MTF **P** is a member of the set of all

possible plants $\{\mathbf{P}\}$ that arise from system uncertainty. The controller $\mathbf{G}$ and prefilter $\mathbf{F}$ are the two degrees of freedom utilised in the QFT control structure. The controller $\mathbf{G}$ is assumed diagonal to simplify the control system synthesis. Due to the zero command input for $y_T(t)$, $F_{11}(s)$ is the only synthesised element in the prefilter. Therefore only two MISO systems need to be considered. The equivalent plants of the MISO systems are $Q_{11}(s)$ for $V_a(t)$ to $\theta(t)$ and $Q_{22e}(s)$ for $V_f(t)$ to $y_T(t)$. The cross-coupling in the MIMO system is represented by the two disturbances $D_{11}(s)$ and $D_{21}(s)$. Using MIMO QFT design method 2 the equivalent plants and disturbances, and the closed loop transfer functions $T_{11}(s)$ and $T_{21}(s)$ resulting from the closure of loop1 and loop2 respectively, are expressed as:

$$T_{11}(s) = \frac{F_{11}(s)G_{11}(s)Q_{11}(s) + D_{11}(s)Q_{11}(s)}{1 + G_{11}(s)Q_{11}(s)}$$

$$T_{21}(s) = \frac{D_{21}(s)Q_{22e}(s)}{1 + G_{22}(s)Q_{22e}(s)} \qquad (5)$$

where,

$$P(s) = [P_{ij}(s)], \quad P^{-1}(s) = [P_{ij}^*(s)], \quad Q_{ij}(s) = 1/P_{ij}^*(s),$$

$$D_{11}(s) = -T_{21}(s)/Q_{12}(s), \quad D_{21}(s) = -F_{11}(s)/Q_{21e}(s).$$

$$Q_{21e}(s) = \frac{Q_{21}(s)(1 + Q_{11}(s)G_{11}(s))}{Q_{11}(s)G_{11}(s)},$$

$$Q_{22e}(s) = P_{22}(s) - \frac{G_{11}(s)P_{21}(s)P_{12}(s)}{1 + G_{11}(s)P_{11}(s)}. \qquad (6)$$

3.3 Frequency Domain Specifications

The time domain specifications are translated to closed-loop frequency domain specifications in the form of the tracking and disturbance bounds. In a QFT design low order bounds typically suffice and are justified if the bounds capture the dominant dynamics of the closed-loop transfer functions over the frequency range where the bounds are enforced. For the single link manipulator low order tracking bounds suffice. Low order disturbance bounds are however ineffective due to problems in the translation of the disturbance specification. These problems are alleviated using a modification of the QFT method as detailed in the forthcoming sections.

Tracking Bound Development; The translation of the tracking specification (S1) is achieved using the traditional QFT approach of an upper and lower bounding 2nd order transfer function, with an additional pole and zero added to increase the allowable uncertainty in the high frequency range. The resulting upper and lower tracking bounds are detailed in equation (13).

Disturbance Bound Development; The translation of the disturbance specification (S2) presents unique difficulties. These stem from two factors; namely the sensitivity of the resulting synthesised controller to the variations in the disturbance bound and the lack

of a priori knowledge of the cross-coupling disturbance dynamics from the rigid mode feedback loop (loop1). The sensitivity function of the resulting Nichols chart bounds on the controller $G_{22}(s)$ to changes in the specified performance bound β_{21} is:

$$S_{B_{D2}}^{G_{22}} = \frac{dG_{22}/G_{22}}{d\beta_{21}/\beta_{21}} = -1 - \frac{1}{g_{22}q_{22e}e^{j(\phi_{22}+\theta_{22e})}} \qquad (7)$$

where $G_{22}(s) = g_{22}e^{j\phi_{22}}$, $Q_{22e}(s) = q_{22e}e^{j\theta_{22e}}$ and the disturbance bound $\beta_{21}(s)$ is magnitude only. For the degenerate case when $\theta_{22e} + \phi_{22} = 0 \pm n \times 360°$, large sensitivity levels occur due to the low authority of the PVDF films. Consequently differences between the dominant dynamics of $\beta_{21}(s)$ and $T_{21}(s)$ have a profound effect on the synthesised controller and the resulting time domain response may be unacceptable. This problem is exacerbated by the lack of a priori knowledge of the cross-coupling disturbance dynamics and control system elements in loop2.

The choice of a 2nd order disturbance bound for the disturbance closed-loop transfer function $T_{21}(s)$ is unacceptable. The principal reason is the presence of two differentiators in the disturbance $D_{21}(s)$. The disturbance is a function of both the prefilter $F_{11}(s)$ and the diagonal controller for loop1 $G_{11}(s)$. Therefore $D_{21}(s)$ can not be known a priori and the choice of a disturbance bound $\beta_{21}(s)$ that captures the dominant dynamics of $T_{21}(s)$ is difficult prior to the closure of loop1.

To overcome the problems in developing the disturbance bound it is proposed that the bound be chosen after loop1 is closed and $Q_{22e}(s)$ and $D_{21}(s)$ are known. This ensures that the dominant dynamics and frequency response (both gain and phase) of the disturbance bound matches that of the closed-loop transfer function $T_{21}(s)$. The difficulty in implementing this proposition is that the design of loop1 requires knowledge of the disturbance bound for loop2 to conservatively upper bound the closed-loop transfer function $T_{21}(s)$. This problem is overcome through the use of QFT MIMO design method 1 to conservatively approximate $T_{21}(s)$ and QFT MIMO design method 2 to formulate the disturbance bound on $T_{21}(s)$. The primary difference between the two methods is that method 2 utilises the knowledge of previously synthesised control elements in the design of the latter loops. Additionally, the proposed method requires that loop1 be closed prior to loop2. The procedure is summarised below:

Design of Loop1; In the design of loop1 $T_{21}(s)$ is conservatively approximated by the closed loop transfer function developed using QFT MIMO design method 1 with $G_{22}(s) = 1$, termed $T_{21}^{(1)}(s)$. Due to the variation in the plants fundamental natural

frequencies several closed-loop transfer functions are developed. The resulting approximation for $T_{21}(s)$ is:

$$T_{21}^{(1)}(\omega_j) = \max_{P \in \{P\}} \left| T_{21(i)}^{(1)}(\omega_j) \right| \qquad (8)$$

$$T_{21(i)}^{(1)}(s) = \frac{-Q_{22(i)}(s)\beta_{11}(s)}{Q_{21(i)}(s)(1 + Q_{22(i)}(s))} \quad ; i \in (1,5) \qquad (9)$$

where $T_{11}(s)$ is conservatively approximated by its upper frequency bound $\beta_{11}(s)$. Importantly, all the elements in $T_{21}^{(1)}(s)$ are known. The design of $G_{11}(s)$ and $F_{11}(s)$, and the closure of loop1 then proceeds.

Design of Loop2; The disturbance bound $\beta_{21}(s)$ for loop2 is now chosen with full knowledge of $D_{21}(s)$ and $Q_{22e}(s)$. The disturbance bound is developed using as a basis the closed loop transfer function from QFT MIMO design method 2 with $G_{22}(s) = 1$:

$$T_{21}^{(2)}(s) = \frac{D_{21}(s)Q_{22e}(s)}{1 + Q_{22e}(s)} \qquad (10)$$

A reduced order model of $T_{21}^{(2)}(s)$ is developed with only the first resonance retained, termed $T_{21R}^{(2)}(s)$. $T_{21R}^{(2)}(s)$ matches the structure and frequency response of $T_{21}^{(2)}(s)$ up to the second resonance. Disturbance bounds are then developed by increasing the damping level of the resonance in $T_{21R}^{(2)}(s)$ until the time-domain disturbance specification S2 is satisfied. This is repeated for each of the plants in the plant set resulting in 5 closed-loop disturbance bounds. The resulting bound $\beta_{21}(s)$ is the maximum magnitude over the frequency responses of all the bounds as detailed in equation (16).

4. QFT CONTROL SYSTEM SYNTHESIS

The frequency domain specifications are detailed below. Specifications F11a and F21a provide stability margins. Specifications F11b and F21b are a result of time domain specifications S1 and S2. Specification F3 is introduced to ensure that, where possible, the design of $G_{11}(s)$ does not introduce additional RHP poles into the equivalent plant for loop2 (Q_{22e}) (Yaniv and Schwartz, 1991).

F11a: $\qquad \left| \dfrac{1}{1 + L_{11}(s)} \right| \leq 5 \, \text{dB} ; \ \omega \geq 0 .$ \qquad (11)

F11b: $\qquad \alpha_{11}(s) \leq |T_{11}(s)| \leq \beta_{11}(s) ; \ \omega \leq \omega_{h1} .$ \qquad (12)

where, $\quad \beta_{11}(s) = \dfrac{3.24(4)}{[0.95:1.8]}, \ \alpha_{11}(s) = \dfrac{1.44}{[1:1.2](4)} .$ \qquad (13)

F21a: $\qquad \left| \dfrac{1}{1 + L_{22}(s)} \right| \leq 5 \, \text{dB} ; \ \omega \geq 0 .$ \qquad (14)

F21b: $\qquad |T_{21}(s)| \leq \beta_{21}(s) ; \ \omega \leq \omega_{h2} .$ \qquad (15)

where, $\quad \beta_{21}(\omega_j) = \max_{P \in \{P\}} \left| \beta_{21_i}(\omega_j) \right| ; i \in (1,6)$ \qquad (16)

F3: $\qquad \left| \dfrac{1}{1 + P_{11}(s)G_{11}(s)} \right| \leq 5 \, \text{dB} ; \ \omega \geq 0 .$ \qquad (17)

In the above, $s = j\omega$, $\beta_{11}(s)$ and $\alpha_{11}(s)$ are the upper and lower tracking bounds and $L_{11}(s) = G_{11}(s)Q_{11}(s)$ and $L_{22}(s) = G_{22}(s)Q_{22e}(s)$ are the loop transmissions for loop1 and loop2 respectively. The frequencies ω_{h1} and ω_{h2} dictate the frequency ranges that the tracking and disturbance rejection specifications must be satisfied. Here $\omega_{h1} = 35$ rad/s and $\omega_{h2} = 50$ rad/s. The bounds $\beta_{21i}(s)$ are the modified $T_{21R}^{(2)}(s)$ with the damping ratio increased to satisfies the time-domain specification S2. An additional bound is added at a frequency higher than the natural frequency of plant1 to account for a shift in the damped natural frequency of plant1 due to over design of $G_{22}(s)$.

The use of MIMO QFT design method 2 requires the selection of the order in which the feedback loops are designed. Loop1 is synthesised first, as the bandwidth required for $G_{11}(s)$ is lower and there is the need to limit over design of $G_{22}(s)$. Designing loop1 first also allows the modified approach for the development of the disturbance bounds to be utilised. The design of the controllers and prefilter was aided through the use of the QFT Toolbox (Borghesani, *et al.*, 1994).

Synthesis of $G_{11}(s)$; The design of $G_{11}(s)$ is relatively simple due to the low levels of variation in the frequency response of equivalent plant $Q_{11}(s)$ in the frequency range from DC to 40 rad/s and the small cross-coupling disturbance from loop2 due to the low authority of the PVDF actuator. The dominating composite bounds on the loop transmission $L_{11}(s)$ are the stability bounds over the range of fundamental frequencies of the plant variants. The synthesised compensator has a bandwidth of 5 rad/s as shown in Fig. 2(a). The controller takes the following form:

$$G_{11}(s) = \frac{1(0.5)}{(0)(17)(1.8)} \qquad (18)$$

Synthesis of $F_{11}(s)$; The prefilter $F_{11}(s)$ is designed to shape the closed loop frequency response to the command input θ_r such that it is contained within the bounds $\alpha_{11}(s)$ and $\beta_{11}(s)$. The cross-coupling disturbance $D_{21}(s)$ in loop2 is directly proportional to the prefilter $F_{11}(s)$ as shown in Eq. (6). Subsequently, the gain of the prefilter is minimised, whilst satisfying the performance bounds, over the range of the plant variants fundamental natural frequencies to reduce the excitation of the fundamental mode of vibration as shown in Fig. 2(a). This reduces the required gain levels and bandwidth of $G_{22}(s)$. The prefilter takes the following form:

$$F_{11}(s) = \frac{1[0.37:0.71][0.34:8]}{(0.49)(4E4)(5E4)[0.84:2.54]} \qquad (19)$$

Synthesis of $G_{22}(s)$*;* The composite stability and performance bounds on the loop transmission $L_{22}(s)$ require a high gain controller due to the low authority of the piezoelectric actuator. This makes the design of $G_{22}(s)$ difficult, with $G_{22}(s)$ likely to have a high bandwidth and subsequent care needed to ensure the effects of the second mode of vibration do not destabilise the system. The trade-off between the design of loop1 and loop2 is therefore evident and the solution is to minimise the prefilter gain over the frequency range of the fundamental natural frequencies of the plant variants. Due to the transparency of the QFT methodology this trade-off is apparent and achievable.

In the design of $G_{22}(s)$ the performance bounds over the frequency range of the plant variants fundamental natural frequencies dominate the controller design. Two lead-lag elements were added to the controller to provide the necessary gain and phase to satisfy the performance bounds over this frequency range. A pole was then added to roll-off the controller gain. A complex pole was then introduced to reduce the phase of the system so the loop transmission passed under the stability boundary before the 2nd mode of vibration. An additional complex pole was then added to roll-off the system response and reduce the bandwidth of the controller. The resulting compensator has a bandwidth of 765 rad/s.

$$G_{22}(s) = \frac{3577(2.106)(2.281)}{(40)(90.74)(121.5)[0.81:20][0.2:42]} \qquad (20)$$

4.1 Frequency Response

The frequency response of the closed-loop transfer functions T_{11} and T_{21} are shown with their respective bounds in Fig. 2. The frequency domain bounds are satisfied by both closed-loop transfer functions over their respective performance bandwidths ω_{h1} and ω_{h2}. The disturbance bound β_{21} is the composite of six bounds, as evident from the six peaks in the bound in Fig. 2(b). The response of plant5, with the highest tip mass and resulting lowest fundamental natural frequency, is exactly that of the bound $\beta_{21}(s)$ up to and around the fundamental natural frequency of plant5. This shows that the higher tip mass case dominates the design and subsequently the other plant cases are slightly over designed, with plant 1 the most over designed. This is the reason for the choice of the sixth disturbance bound in the formation of $\beta_{21}(s)$.

Notably, the frequency response of all the five closed-loop transfer functions essentially satisfy both the gain and phase bounds imposed by $\beta_{21}(s)$ as shown in Fig. 2(c). This is despite only the magnitude bounds being enforced through the QFT design. Hence the designer can be confident of a good time-to-frequency domain mapping and acceptable time domain responses.
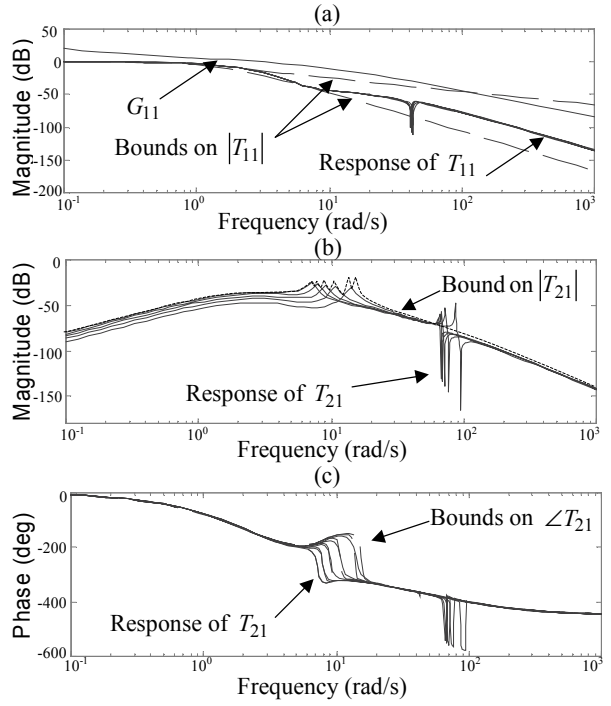
Fig. 2. Simulated Frequency Response (a) Bounds on $|T_{11}(s)|$, Magnitude Response of $T_{11}(s)$ and $G_{11}(s)$, (b) Bound on $|T_{21}(s)|$, Magnitude Response of $T_{21}(s)$, (c) Bounds on $\angle T_{21}(s)$, Phase Response of $T_{21}(s)$.
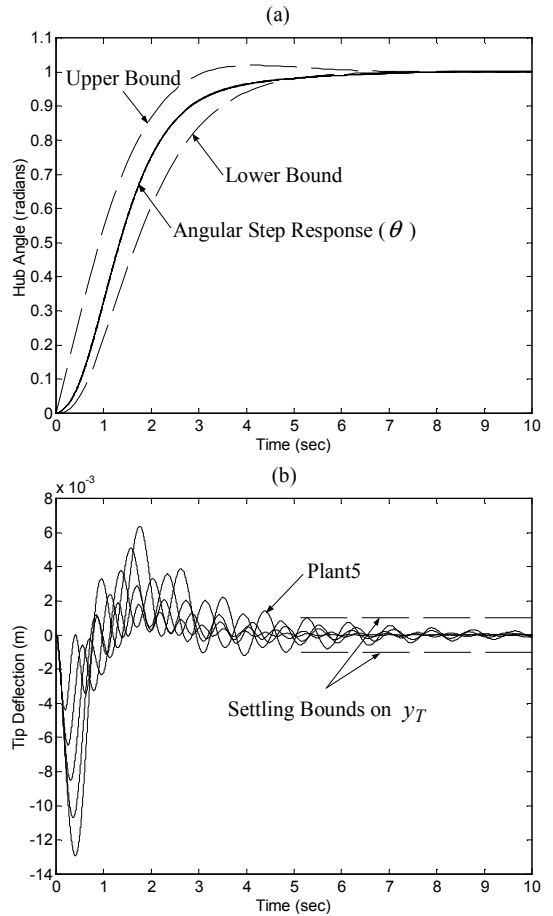
Fig. 3: Time domain response to a command step input: (a) Hub Angle Step Response, (b) Tip Displacement

5. RESULTS AND DISCUSSION

The simulated time domain responses are shown in Fig. 3. The robustness of the QFT designed control system is evident, with the time-domain performance specifications S1 and S2 satisfied for all plants in the plant set. It should be noted that no tuning of the controllers was performed to demonstrate the efficacy of the QFT methodology. However, experience with the system aided in the choice of sensible time-domain specifications S1 and S2.

The tracking response is acceptable with $\theta_{e(\max)}\big|_{t\geq 5s} \leq 0.02$ rad. The disturbance rejection is acceptable with $y_{T(\max)}\big|_{t\geq 5s} = 0.001$ m, which is the design specification. Notably there is no conservatism in the response of plant5, showing the advantage of choosing a bound that accurately matches both the structure and frequency response of the dominant system dynamics over frequency range of the performance specifications. Through the use of the modified approach for the development of the disturbance bound, the time and frequency domain specifications are satisfied. But more importantly, the time and frequency domain specifications are barely satisfied, thus implying that the translation to the frequency domain is not conservative. The conservatism in the satisfaction of the bounds for the lower tip mass plants, and thus the controller bandwidth, can be reduced by designing a controller of higher order so that the loop transmission is closer to the bounds. Clearly the designer can see the trade-off between controller complexity, over design and controller bandwidth. Evidently, the use of the modified method to develop the disturbance bound for this high-low authority system is effective and provides a good mapping between the time and frequency domain.

The simulated control voltages for the DC motor are below the saturation level of 24V. The voltage levels for the PVDF actuator are above the saturation level of 200V with a maximum level of 300V. The response of the system with the saturation constraint imposed is not shown, as this would invalidate the QFT design. The controller $G_{22}(s)$ was designed to be unconditionally stable and therefore the effects of saturation will not destabilise the system response but will result in a small increase in the settling time.

6. CONCLUSION

The QFT methodology was employed to synthesise a control system to satisfy quantitative time domain specifications on the tip position of a hybrid actuated single-link manipulator. Specific difficulties in the development of performance bounds for the regulation of cross-coupling disturbances were found to dominate the design. These difficulties were addressed using a proposed modification to the classical method of disturbance bound development utilising QFT MIMO methods 1 and 2. This identifies issues in the bounding of closed-loop transfer functions that are relevant to MIMO designs employing frequency domain bounds.

Simulation of the step response demonstrated the achievement of quantitative time domain specifications on the position of the manipulator over the range of plant uncertainty. The quantitative aspects of the QFT methodology resulted in a control system that satisfied the performance specifications with low bandwidth and relatively low order compensators. The transparency of the QFT synthesis method highlighted the design limitations imposed by the system uncertainties and the fundamental trade-off between fast rotational motion and low levels of tip deflection. This naturally led to the design of the prefilter to minimise the effect of fast rotation on the manipulator whilst satisfying the QFT design constraints. Current research aims to overcome difficulties in the QFT design arising from the inclusion of additional modes of vibration and experimentally verify the controller performance.

7. REFERENCES

Book, W. J. (1990). Modelling, Design, and Control of Flexible Manipulator Arms: A Tutorial Review. *Proceedings of the 29th Conference on Decision and Control*, Honolulu, Hawaii, 500-506.

Borghesani, C., Y. Chait and O. Yaniv (1994). Quantitative Feedback Theory Toolbox Users Guide, The Math Works Inc., Natick, MA.

Chang, P. and S. Jayasuriya (1995). An Evaluation of Several Controller Methodologies Using a Rotating Flexible Beam as a Test Bed. *ASME Journal of Dynamic Systems, Measurement and Control*, **117**, 360-373.

Choi, S., S. Cho, H. Shin, and H. Kim (1999) Quantitative Feedback Theory Control of a Single-link Flexible Manipulator Featuring Piezoelectric Actuator and Sensor. *Smart Material and Structures*, **8**, 338-349.

Gu, M. and S.F. Asokanthan (1999). Combined Discrete-distributed Control of a Slewing Flexible Manipulator: Theory and Experiments. *Proceedings of the 14th World Congress of IFAC*, Beijing, P. R. China, 83-88.

Horowitz, I. (1991). Survey of Quantitative Feedback Theory (QFT). *International Journal of Control*, **53**, No. 2, 255-291.

Houpis, C.H. and S.J. Rasmussen (1999). *Quantitative Feedback Theory*. Marcel Dekker Inc., NY.

Yang, S.M. and Y.C. Liu (1995). Frequency domain control of flexible beams with piezoelectric actuator. *ASME Journal of Dynamic Systems, Measurement and Control*, **117**, 541-546.

Yaniv, O. and I. Schwartz (1991). Criterion for loop stability in MIMO feedback systems having an uncertain plant. *International Journal of Control*, **53**, No. 3, 527-539.